

Towards the Algorithmic Molecular Self-assembly of Fractals by Cotranscriptional Folding^{*}

Yusei Masuda, Shinnosuke Seki, and Yuki Ubukata

Department of Computer and Network Engineering, The University of Electro-Communications, 1-5-1, Chofugaoka, Chofu, Tokyo, 1828585, Japan
s.seki@uec.ac.jp

Abstract. RNA cotranscriptional folding has been recently proven capable of self-assembling a rectangular tile *in vitro* (RNA origami). The oritatami system is a novel computational model of cotranscriptional folding. In this paper, we initiate the theoretical study on the algorithmic self-assembly of shapes by cotranscriptional folding using the oritatami system. We propose an oritatami system that folds into an arbitrary finite portion of the Heighway dragon, which is a fractal also-known as the paperfolding sequence $P = RRLRLLLR \cdots$. The i -th element of P can be obtained by feeding i in binary to a 4-state deterministic finite automaton with output (DFAO). We implement this DFAO and a bit-sequence bifurcation component as modules of oritatami system. Combining them with a known binary counter module yields the proposed oritatami system.

1 Introduction

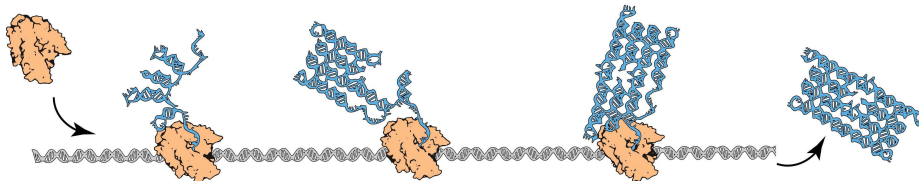


Fig. 1. RNA cotranscriptional folding. An RNA polymerase enzyme attaches to a template DNA sequence (gray spiral), scans it through, and synthesizes its RNA copy. The RNA sequence begins to fold upon itself immediately as it emerges from the RNA polymerase.

^{*} This work is in part supported by JST Program to Disseminate Tenure Tracking System, MEXT, Japan, No. 6F36 and by JSPS KAKENHI Grant-in-Aid for Young Scientists (A) No. 16H05854 to S. S.

An RNA sequence, over nucleotides of four kinds A, C, G, U, is synthesized (*transcribed*) from its template DNA sequence over A, C, G, T nucleotide by nucleotide by an RNA polymerase (RNAP) enzyme according to the one-to-one mapping $A \rightarrow U$, $C \rightarrow G$, $G \rightarrow C$, and $T \rightarrow A$ (for details, see, e.g., [2]). The yield, called *transcript*, starts folding immediately after it emerges from RNAP. This is the *cotranscriptional folding*. Geary, Rothmund, and Andersen have recently demonstrated the capability of cotranscriptional folding to manufacture an RNA molecule of an intended shape at nano-scale [7]. They actually proposed an architecture of a DNA sequence whose transcript folds cotranscriptionally into an RNA rectangular tile highly likely *in vitro* (see Figure 1).

Using a novel computational model of cotranscriptional folding called the *oritatami system* [6], we shall initiate the theoretical study on algorithmic self-assembly of shapes by cotranscriptional folding. Algorithms and computation are fundamental to molecular self-assembly as illustrated in an enormous success of their use in DNA tile self-assembly (see, e.g., [4, 13, 17] and references therein). A fractal pattern called Sierpinski triangle was algorithmically self-assembled from coalescence of DNA tiles that compute XOR [15]. Cotranscriptional folding exhibits highly sophisticated computational and algorithmic behaviors. Fluoride riboswitches in the *Bacillus cereus* bacteria cotranscriptionally fold a terminator stem that suppresses gene expression or not, depending on ligand concentration [16]. Cotranscriptional folding is in fact proved Turing-universal by the oritatami system [5]. The Turing-machine simulator is gigantic and intricate but oritatami systems have implemented basic computational devices such as binary counter [6] as a module comparable in size to the gene expression regulator. The binary counter module consists of half-adder components, which fold into one of possible four conformations depending on a 1-bit input and a 1-bit carry/non-carry encoded in their surroundings somehow. It can be diverted as a copier for binary sequences by being fed with the non-carry. They shall be reused in this paper.

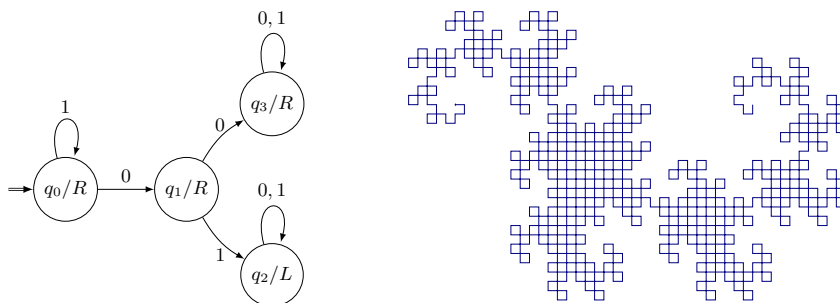


Fig. 2. Highway dragon. (Left) A DFAO that reads the binary representation of i from the least significant bit and outputs the direction to turn. (Right) The 10th iteration of the Highway dragon, that is, the first $2^{10} - 1$ turns of it.

Algorithmic cotranscriptional folding of Sierpinski triangle would allow oritatami systems to borrow rich insights from the DNA tile self-assembly. On the other hand, in order to cut more directly to the heart of algorithmic self-assembly by cotranscriptional folding, we should study the fabrication of shapes that is traversable in some algorithmic way. One such way is to feed a turtle program (see [1]) with a binary *automatic sequence* as commands (drawing a line segment, rotation, etc.), whose i -th bit (starting from 0) can be obtained by giving a binary representation of i from the least significant bit to one deterministic finite automaton with output (DFAO) [3]. Shapes thus describable include the Heighway dragon [3] and von Koch curve [10]. A DFAO for the Heighway dragon is shown in Figure 2 (Left). It is to read the binary representation of $i \geq 0$ from the least significant bit (LSB) and outputs the i -th direction $P[i]$ to turn (R or L) assigned to the state finally reached as follows:

$$\begin{array}{ccccccc} i & = & 0 & 2 & 6 & 14 & 30 \dots \\ P[i] & = & R & RL & RRLL & RRLLRLL & RRLLRLLLRLLRLL \dots \end{array}$$

where only the values of i at the end of the first five iterations are specified. A turtle should interpret an R (resp. L) as “move forward by unit distance and turn right (resp. left) 90 degrees.” The sequence is denoted by P after its appellative *paperfolding sequence* [3].

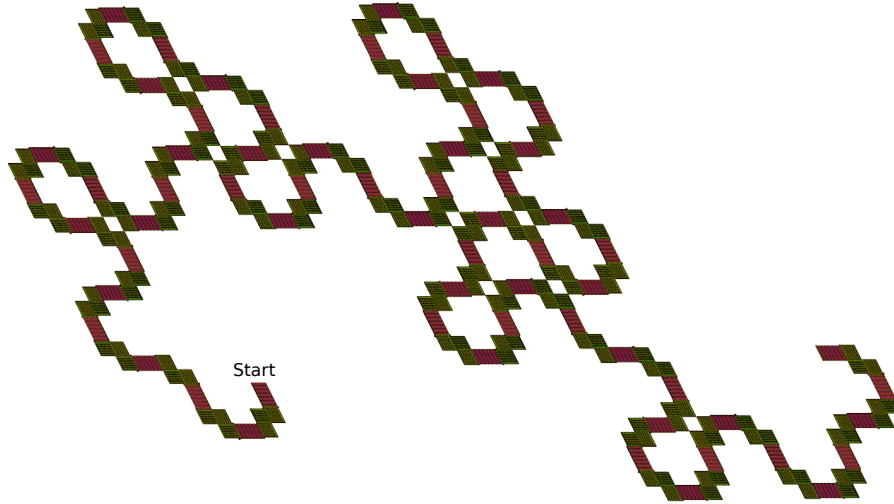


Fig. 3. The 6th iteration of the Heighway dragon folded by the proposed oritatami system.

In this paper, we propose an oritatami system that cotranscriptionally folds into a finite portion of the Heighway dragon. Figure 3 shows the 6-th iteration of

the Highway dragon thus folded (the dragon is slanted, but this is because the oritatami system operates on the triangular grid). The system consists of four modules: binary counter and copier modules, which are a technical modification of those from [6], DFAO module, and turning module. A (red) line segment in Figure 3 consists of a binary counter and copiers, which increment the current count i by 1 and let the count be propagated through. At the end of the segment is a DFAO module, which computes $P[i]$, the direction to turn, while forwarding the count i from the last copier to the following turning module. A (green) L-shaped block is the turning module. A turning module consists of three rhombic components, each of which bifurcates the count i and the direction $P[i]$ leftward as well as rightward and directs the growth of further folding leftward if $P[i] = L$ or rightward if $P[i] = R$. We shall implement the DFAO and turning modules and verify them.

A JavaScript program to execute this oritatami system and websites on which this program is executable are freely available [11].

2 Preliminaries

Let Σ be a set of types of abstract molecules, or *beads*, and Σ^* be the set of finite sequences of beads. A bead of type $a \in \Sigma$ is called an a -bead. Let $w = b_1 b_2 \cdots b_n \in \Sigma^*$ be a string of length n for some integer n and bead types $b_1, \dots, b_n \in \Sigma$. The *length* of w is denoted by $|w|$, that is, $|w| = n$. For two indices i, j with $1 \leq i \leq j \leq n$, we let $w[i..j]$ refer to the subsequence $b_i b_{i+1} \cdots b_{j-1} b_j$; if $i = j$, then we simplify $w[i..i]$ as $w[i]$. For $k \geq 1$, $w[1..k]$ is called a *prefix* of w .

Oritatami systems fold their transcript, a sequence of beads, over the triangular grid as suggested in Figure 4 cotranscriptionally based on hydrogen-bond-based interactions (*h-interactions* for short) which the rule set of the system allow for between adjacent beads of particular types. Let $\mathbb{T} = (V, E)$ be the triangular grid graph. A directed path $P = p_1 p_2 \cdots p_n$ in \mathbb{T} is a sequence of *pairwise-distinct* points $p_1, p_2, \dots, p_n \in V$ such that $\{p_i, p_{i+1}\} \in E$ for all $1 \leq i < n$. Its i -th point is referred to as $P[i]$. A *rule set* $\mathcal{H} \subseteq \Sigma \times \Sigma$ is a symmetric relation over the set of pairs of bead types, that is, for all bead types $a, b \in \Sigma$, $(a, b) \in \mathcal{H}$ implies $(b, a) \in \mathcal{H}$.

A *conformation* C is a triple (P, w, H) of a directed path P in \mathbb{T} , $w \in \Sigma^*$ of the same length as P , and a set of h-interactions $H \subseteq \{\{i, j\} \mid 1 \leq i, i+2 \leq j, \{P[i], P[j]\} \in E\}$. This is to be interpreted as the sequence w being folded in such a manner that its i -th bead $w[i]$ is placed on the i -th point $P[i]$ along the path and there is an h-interaction between the i -th and j -th beads if and only if $(i, j) \in H$. The condition $i+2 \leq j$ represents the topological restriction that two beads next to each other along the path cannot form an h-interaction between them. Let \mathcal{H} be a rule set. An h-interaction $(i, j) \in H$ is *valid with respect to* \mathcal{H} , or simply *\mathcal{H} -valid*, if $(w[i], w[j]) \in \mathcal{H}$. This conformation is \mathcal{H} -valid if all of its h-interactions are \mathcal{H} -valid. For an integer $\alpha \geq 1$, this conformation is of *arity* α if the maximum number of h-interactions per bead is α , that is, if for any $k \geq 1$, $|\{i \mid (i, k) \in H\}| + |\{j \mid (k, j) \in H\}| \leq \alpha$ and this inequality holds as an

equation of some k . By $\mathcal{C}_{\leq \alpha}$, we denote the set of all conformations of arity at most α .

Oritatami systems grow conformations by elongating them under their own rule set. Given a rule set \mathcal{H} and an \mathcal{H} -valid finite conformation $C_1 = (P, w, H)$, we say that another conformation C_2 is an *elongation of C_1 by a bead $b \in \Sigma$* , written as $C_1 \xrightarrow{\mathcal{H}}_b C_2$, if $C_2 = (Pp, wb, H \cup H')$ for some point p not along the path P and set of h-interactions $H' \subseteq \{\{i, |w| + 1\} \mid 1 \leq i < |w|, \{P[i], p\} \in E, (w[i], b) \in \mathcal{H}\}$, which can be empty. Note that C_2 is also \mathcal{H} -valid. This operation is recursively extended to the elongation by a finite sequence of beads as: for any conformation C , $C \xrightarrow{\mathcal{H}}_{\lambda}^* C$; and for a finite sequence of beads $w \in \Sigma^*$ and a bead $b \in \Sigma$, a conformation C_1 is elongated to a conformation C_2 by the sequence wb , written as $C_1 \xrightarrow{\mathcal{H}}_{wb}^* C_2$, if there is a conformation C' that satisfies $C_1 \xrightarrow{\mathcal{H}}_w^* C'$ and $C' \xrightarrow{\mathcal{H}}_b C_2$.

A finite *oritatami system* is a 5-tuple $\Xi = (\mathcal{H}, \alpha, \delta, \sigma, w)$, where \mathcal{H} is a rule set, α is an arity, $\delta \geq 1$ is a parameter called the *delay*, σ is an initial \mathcal{H} -valid conformation of arity α called the *seed*, upon which its finite *transcript* $w \in \Sigma^*$ is to be folded by stabilizing beads of w one at a time so as to minimize energy collaboratively with the succeeding $\delta - 1$ nascent beads. The energy of a conformation $C = (P, w, H)$, denoted by $\Delta G(C)$, is defined to be $-|H|$; the more h-interactions a conformation has, the more stable it gets. The set $\mathcal{F}(\Xi)$ of conformations *foldable* by this system is recursively defined as: the seed σ is in $\mathcal{F}(\Xi)$; and provided that an elongation C_i of σ by the prefix $w[1..i]$ be foldable (i.e., $C_0 = \sigma$), its further elongation C_{i+1} by the next bead $w[i + 1]$ is foldable if

$$C_{i+1} \in \arg \min_{C \in \mathcal{C}_{\leq \alpha} \text{ s.t. } C_i \xrightarrow{\mathcal{H}}_{w[i+1]} C} \min \left\{ \Delta G(C') \mid C \xrightarrow{\mathcal{H}}_{w[i+2..i+k]}^* C', k \leq \delta, C' \in \mathcal{C}_{\leq \alpha} \right\}. \quad (1)$$

We say that the bead $w[i + 1]$ and the h-interactions it forms are *stabilized* according to C_{i+1} . Note that an arity- α oritatami system cannot fold any conformation of arity larger than α . A conformation foldable by Ξ is *terminal* if none of its elongations is foldable by Ξ .

The oritatami system Ξ is *deterministic* if for all $i \geq 0$, there exists at most one C_{i+1} that satisfies (1). Thus, a deterministic system folds into a unique terminal conformation. Let us provide an example of deterministic oritatami system that folds into a motif of great use called the *glider*.

Example 1. Let $\Sigma = \{a, a', b, b', \bullet\}$. Consider a delay-3 oritatami system whose seed is colored in red in Figure 4 (left), transcript is a repetition of $a \bullet b' b \bullet a'$, and the rule set is $\mathcal{H} = \{(a, a'), (b, b')\}$, which makes \bullet -beads inert.

By the fragment $a \bullet b'$ of the first three beads of the transcript, the seed can be elongated in many ways; three of them are shown in Figure 4 (left). The only bead on the fragment capable of a new h-interaction is b' (with a b -bead). In order for the b' -bead to form an h-interaction with a b -bead, the first a -bead must be located to the east of the last bead of the seed. Thus, the a -bead is

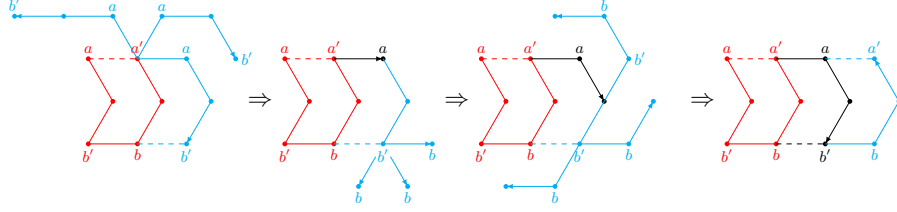


Fig. 4. Progression of a glider by distance 1.

stabilized there. The next bead is then transcribed, which is of type b . It is not capable of any h-interaction because any b' around is either too far or too close. Hence, the nascent fragment $\bullet b'b$ gets stabilized as being folded as done before up to at least the first two beads. The \bullet bead is stabilized southeastward. An inert bead pops up next so that the b' gets stabilized southwestward as suggested before. The first three beads a, \bullet, b' have been thus stabilized and the glider has moved forward by unit distance. It is easily induced inductively that gliders of arbitrary “flight distance” can be folded.

Gliders also provide a medium to propagate 1-bit straight at arbitrary distance. The height (top or bottom) of the first bead determines whether the last bead is stabilized top or bottom after flying a given distance. For instance, the glider in Figure 4 launches top and thus its last bead (the a') also comes top after traveling the distance 2. The oritatami system we shall propose exploits this information-carrying capability.

3 Highway dragon oritatami system

We propose a generic design of deterministic oritatami system that allows us to fold an arbitrary finite portion of the Highway dragon. The design concept has been already explained in the introduction. The dragon it folds into is actually slanted as illustrated in Figure 3, which is more natural than the conventional (upright) one to be folded over the triangular grid. The design sets both delay and arity to 3 and employs a fixed number of bead types (about 2000), no matter which portion is folded. Minimizing the number of bead types has just proven NP-hard [8].

Any finite portion of the Highway dragon is expected to be foldable by *hard-coding* if an arbitrary number of bead types is available and the shape can be scaled-up (though, if rescaling is not allowed, it is NP-hard to decide if for a given finite shape, there exists an oritatami system that folds into the shape [14]). The proposed design cannot take this approach because the number of bead types available is fixed. An oritatami system $\Xi = (\mathcal{H}, \alpha, \delta, \sigma, w)$ that the design provides is periodic in the sense that its transcript is a periodic sequence. If this system is for the n -th repetition of the Highway dragon, then the length of its period is $|w|/2^{n-1}$. One period corresponds to a successive two pairs of a red line segment and the following green L-shaped block.

Why do these two pairs have to be distinguished from each other? The answer to this question lies in the fact that the Highway dragon is slanted. The slanted dragon involves two types of left turn as well as two types of right turn: acute and obtuse. Capability of one turning module to make all of the four possible turns would shorten the period by half. Such a turning module, however, would have to take quite a large number of conformations; recall that what the module has to turn is not a straw but a thick wire which bears the current count i . Implementing such a module totally ignores the level of oritatami design techniques accumulated so far. Our approach makes it sufficient to implement a turning module capable of just an acute turn and an obtuse turn. Observe that after the (slanted) vertical segment, certainly the left turn is obtuse while the right turn is acute, whereas after the horizontal segment, the left turn is acute while the right turn is obtuse. In addition, we know *a priori* which segments are vertical and which are horizontal; indeed vertical segments and horizontal segments occur alternately on the Highway dragon. Therefore, we can attach a proper interpreter to a DFAO module to convert its output L/R into a signal A(cute)/O(btuse). Two types of interpreters are hence needed: vertical interpreter converts L into obtuse and R into acute, while horizontal one converts them the other way around.

The sole difference between the first and second halves of a period is anyway the type of interpreter (AO or AO). Thus, it should be sufficient to explain only the first half. The half consists of four subsequences for the counter, copier, DFAO, and turning modules. It folds as abstracted in Figure 5 into one line segment plus one turn of the Highway dragon and has its four modules accomplish the following processes, respectively:

1. $i \leftarrow i + 1$ (count-up)
2. Copy i (drawing a line segment)
3. Compute $P[i]$
4. Make a turn according to $P[i]$

Its length is proportional to n^2 and hence so is the length of a period. The seed of the system replaces the counter module at the beginning of the first period and encodes the initial value of i as a sequence of bead types in an appropriate format such that copier modules can “read” the count i . We shall explain how modules read something in Section 3.1. Before explaining the implementation of each module, we should point out one significant issue specific to the folding by oritatami systems. It rises when the Highway dragon makes a turn where it has already made another turn before, that is, when two turns share a point. By definition, oritatami systems cannot put a bead anywhere occupied by another bead. This is the reason of the L-shape of the turning module. As shown in Figures 3 and 5, the proposed system makes an acute turn by having three bifurcation components direct the growth of further folding acutely one after another, while an obtuse turn by having them direct the growth rather obtusely.

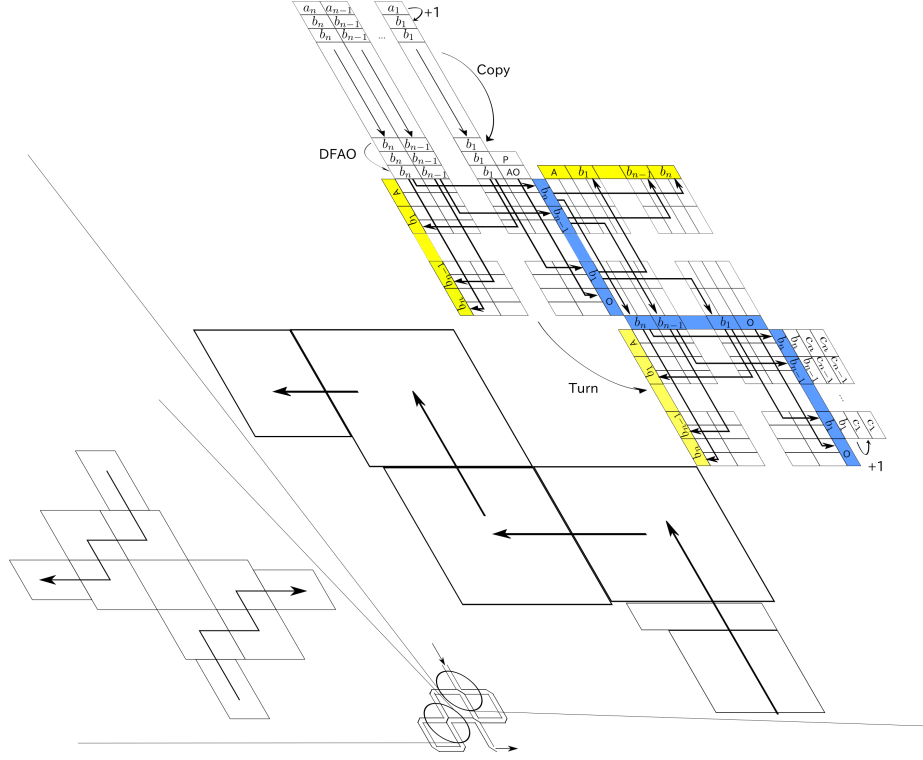


Fig. 5. Folding of one segment plus turn of the Highway dragon, flow of information through it, and two ways of collision avoidance between two turns.

3.1 Modules

Now it suffices to explain how modules and their components are implemented, interlocked with each other, and collaborate. Using the simulator developed for [9], we have verified that all of the components fold correctly in all possible environments, which are abstracted in Figures 5, 7, and 13.

Counter and copier modules The existing binary counter [6] was modified so as to operate in the dynamics (1), which is more prevailing [5, 8, 9, 12] but less tractable than the one the original counter used.

The essential component of this module is the half-adder. In Figure 5, half-adder components are abstracted as small rhombuses at the top labeled with a_n, a_{n-1}, \dots, a_1 , where the one with a_j is for the j -th bit of the current count i . Though not described, two horizontally adjacent half-adders sandwich a glider of even length as a space to keep them away from each other sufficiently to prevent any undesirable interference. Figure 6 illustrates its four possible conformations. The whole oritatami system is designed in such a manner that a

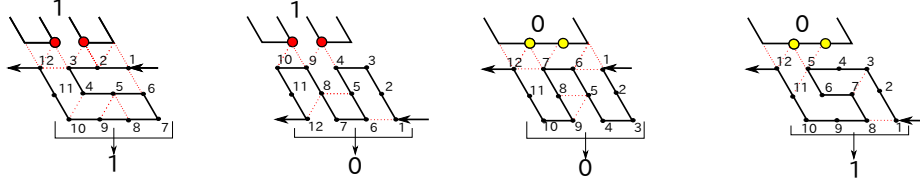


Fig. 6. All conformations of the half-adder component.

1-bit input (1 or 0) is exposed to the specific position (colored red or yellow in Figure 6) as a pair of bead types by the previous turning module. The system is also designed in such a manner that a half-adder starts folding either at the top, as in the first and third conformations, or at the bottom as in the other two. The half-adder considers the top start position as non-carry and the bottom start position as carry. Thus, only when a half-adder takes 1 and carry, it ends at the bottom (second conformation in Figure 6), which is propagated to the next half-adder as it is via the spacer between them. These four conformations expose sequences of four bead types below that are distinct enough to convey the intended 1-bit output to another computing component, or in other words, we can design a component that can “read” the output. From this point forward, conformations for other components will be illustrated; their input and output will be labeled by their meaning mutually understood by the components that exchange them.

Being fed with non-carry, the counter module serves as the copier module. Combining them one after another yields a line segment of arbitrary length, through which the current count i is propagated.

DFAO module A DFAO module receives the current count i from the last copier module, computes $P[i]$, interprets it properly either A or O, and outputs it together with the count i at the very end of a red line segment.

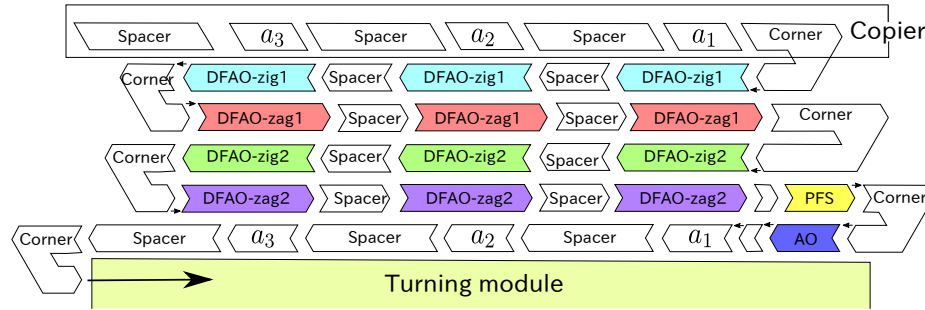


Fig. 7. Component-level abstraction of the folding of DFAO module.

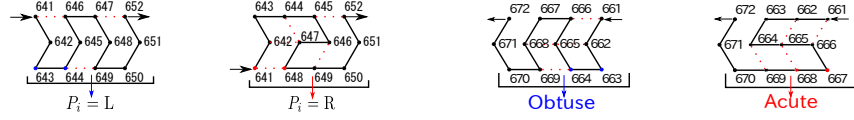


Fig. 8. (left) The possible two conformations of PFS: PFS-L, PFS-R. (right) The possible two conformations of AO.

DFAO is composed of the six components: DFAO-zig, DFAO-zag1, DFAO-zig2, DFAO-zag2, PFS, AO (or “ $\overline{\text{AO}}$ ”). At the component-level, it folds into two zig-zags as abstracted in Figure 7. What the module does in the first zig-zag is to have DFAO-zig1s and DFAO-zag1s read the current count i from its LSB and “mark” the first 0, while propagating i . In the second zig-zag, it employs DFAO-zig2s and DFAO-zag2s to check whether the automaton transitions to the state q_2 ($P_i = L$) or else ($P_i = R$). The second zag is to end at the top if $P_i = L$ or at the bottom if $P_i = R$. PFS takes one of the two conformations in Fig. 8 and outputs P_i downward. In vertical segments, PFS is followed by AO, while in horizontal segments, it is followed by $\overline{\text{AO}}$. AO interprets the PFS’ output $P_i = R$ as acute and $P_i = L$ as obtuse, as shown in Fig. 8. $\overline{\text{AO}}$ interprets them the other way around. Let us explain briefly how each of the components folds to fulfill its roles.

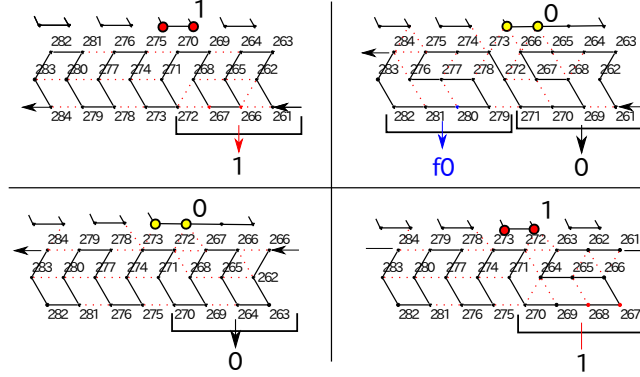


Fig. 9. The possible four conformations of DFAO-zig1: (top) Dzig1-1 and Dzig1-f0; (bottom) Dzig1-20 and Dzig1-21.

DFAO-zig1’s collaboratively detect the first 0 in two phases. Phase1 is to copy all the 1’s before the first 0 and Phase2 is to copy all the bits after the first 0. These phases are distinguished by the relative position at which a DFAO-zig1 starts folding to the copier above (in Phase1 it is at the bottom, while in Phase2 it is at the top, as suggested in Figure 9). In Phase1, DFAO-zig1s certainly take the conformation Dzig1-1 (the top left conformation in Figure 9). In Phase1, if the half-adder above outputs 0, this is the first 0. Then the DFAO-

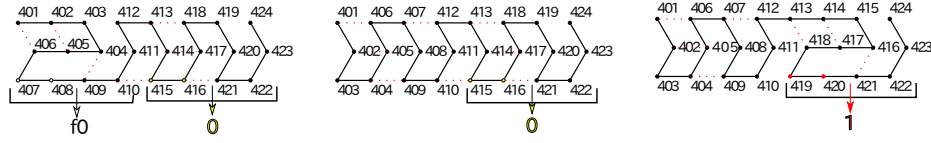


Fig. 10. The possible three conformations of DFAO-zag1: Dzag1-f0, Dzag1-0, and Dzag1-1 from left.

zig1 takes the conformation Dzig1-f0 instead, ending at the top to transition to Phase 2. Each of the succeeding DFAO-zig1s takes one of the other two conformations Dzig1-20 and Dzig1-21 to copy all the remaining bits. Note that there is a cushion between two DFAO-zig1s called *spacer*. Spacers have been already used to prevent undesirable interference among components. They are implemented as a glider (see Example 1), hence capable of propagating 1bit on which phase the system is in. In the first zag, DFAO-zag1's just propagate 0's, 1's, and the first 0 by taking the proper one of the three conformations in Figure 10.

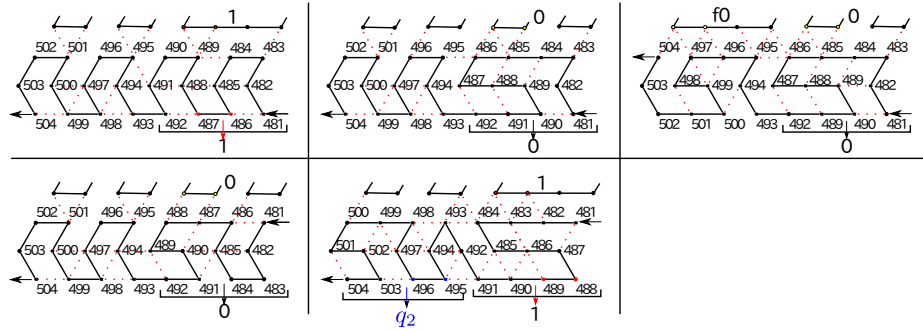


Fig. 11. The possible five conformations of DFAO-zig2: (top) Dzig2-1, Dzig2-0, Dzig2-f0, (bottom) Dzig2-f00, and Dzig2-f01.

In the second zig, DFAO-zig2's check whether the first 0 is followed by 0 or 1, being read from LSB. They first copy all the 1's up to the first 0 by taking the conformation Dzig2-1 (top left in Figure 11). The next letter is the first 0, which is distinguished from other 0's by the special conformation Dzag1-f0 of the DFAO-zag1 responsible for the bit, or more precisely, by its marker f0. Starting at the bottom and reading 0, the DFAO-zig2 can take two conformations Dzig2-0 and Dzig2-f0. These conformations share the first half. The marker f0 folds the second half so as to end at the top, yielding Dzig2-f0. The next DFAO-zig2 therefore starts to fold at the top so that it takes one of the two conformations Dzig2-f00 and Dzig2-f01 depending on the bit read. Recall that reading 1 here is equivalent to transitioning to q_2 , that is, $P[i] = L$. Observe that Dzig2-f01 is

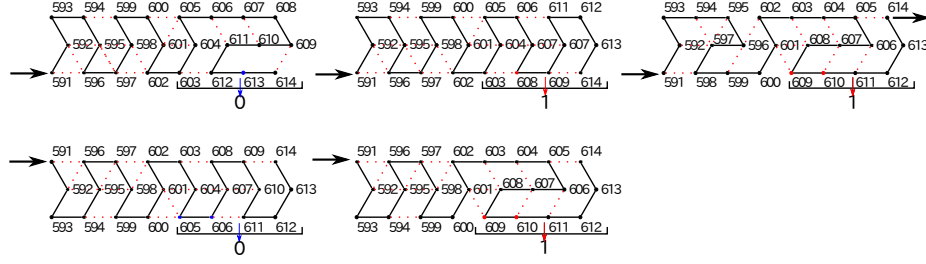


Fig. 12. The possible five conformations of DFAO-zag2: (top) Dzag2-L0, Dzag2-L1, Dzag2-T1, (bottom) Dzag2-R0, and Dzag2-R1.

provided with the marker q_2 , which lets the DFAO-zag2 component below know $P[i] = L$. These conformations end at the bottom. The remaining 0's and 1's are copied by Dzig2-0 and Dzig2-1, respectively. The second zag starts at the bottom and copy 0's and 1's by the two conformations Dzag2-L0 and Dzag2-L1 of DFAO-zag2 (top left and center in Figure 12) until a DFAO-zag2 encounters a 1, or more precisely, its marker q_2 , if any. Such DFAO-zag2 takes the special conformation Dzag2-T1 and changes the ending position to the top, letting the remaining DFAO-zag2s rather take Dzag2-R0 and Dzag2-R1 for copying, which end at the top. As such, the second zag can feed $P[i]$ to PFS as explained before, while propagating the current count i .

The third zig lets $P[i]$ go through its AO (or \overline{AO}) component to be reinterpreted either as A(cute) or as O(btuse) and propagates the current count i .

Turning module Lastly, we explain the turning module. It consists of two parts: bit-sequence bifurcation submodule and steering arm component (colored in blue in Figure 13).

The bifurcation submodule sends bits of the current count i and the reinterpreted signal (A or O) as shown in Figure 5 while folding into zig-zags. For that, it employs the following four types of components:

1. components to propagate 1-bit vertically: body-rpx (Figure 14), body-lpx1 (Figure 15), body-lpx2 (Figure 16);
2. a component to let 1-bit cross another 1-bit: body-gx (Figure 17);
3. components to fork 1-bit vertically and horizontally: body-rgy (Figure 18) and body-lgy (Figure 19);
4. components to undergo transition between a zig and a zag and exposes 1-bit outside: turn-rgp (Figure 20) and turn-lgp (Figure 21).

The first two types have already been implemented (see, e.g., [9]) so that we shall explain the others.

The component body-rgy takes one of the two conformations in Figure 18 depending on the 1-bit encoded in the two beads above. Output below, the 1-bit is encoded as a type of the second bead from left, while output right, it is

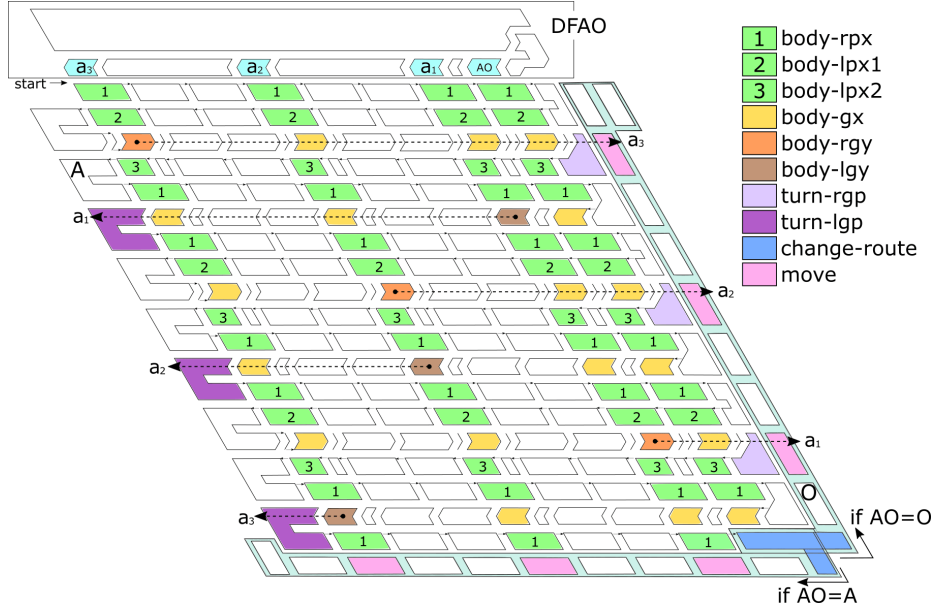


Fig. 13. Component-level abstraction of folding of turning module. All the white components in the middle are spacers, some of which are implemented in the shape of parallelogram instead of glider.

encoded as the position of its last bead (top or bottom). Its zag-variant, body-lyg, is implemented analogously; for its conformations.

The 1bit forked rightward by a body-rgy transfers till the end of the zig without being jammed because all remaining modules in the zig are designed in such a way that they start and end at the same height like the even-distance glider. The module turn-rgp receives the 1bit (top or bottom), and exposes it by taking one of the two conformations in Figure 20. The module turn-lgp functions analogously in zags as being folded in Figure 21.

The bifurcation submodule also propagates the 1-bit A or O, output by the DFAO, to tell the steering arm which way it should take. Specifically, the signal has the first module, change-route, of the steering arm take one of the two conformations in Figure 22, guiding the rest of the steering arm towards the ordered direction. The steering arm is provided with move modules (Figure 23), which let bits of the bifurcated bit sequence pass through. Note that the turning module does not have to bifurcate AO. Indeed, the second and third turning modules are supposed to turn in the same manner as the first one. It hence suffices to append A and O to the bifurcated bit sequences on the acute side and obtuse side, respectively, as shown in Figure 13.

Remark 1. In fact, as suggested in Figure 13, the bifurcation component outputs an input bit sequence also downward. That is, it bifurcates the sequence into

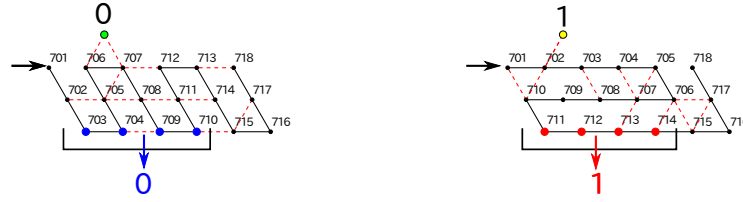


Fig. 14. The possible two conformations of body-rpx component.

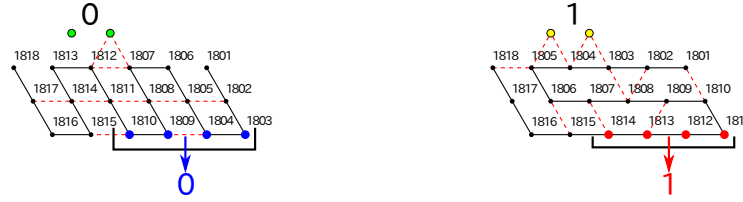


Fig. 15. The possible two conformations of body-lpx1 component.

three ways. This provides a more space-efficient way to replicate a bit sequence many-folds.

Acknowledgements

We would like to thank Hwee Kim and Aleck Johnsen for their helpful advices and discussions.

References

1. Harold Abelson and Andrea diSessa. *Turtle Geometry The Computer as a Medium for Exploring Mathematics*. MIT Press Series in Artificial Intelligence. The MIT Press, 1981.
2. Bruce Alberts, Alexander Johnson, Julian Lewis, David Morgan, Martin Raff, Keith Roberts, and Peter Walter. *Molecular Biology of the Cell*. Garland Science, 6th edition, 2014.
3. Jean-Paul Allouche and Jeffrey Shallit. *Automatic Sequences: Theory, Applications, Generalizations*. Cambridge University Press, 2003.
4. David Doty. Theory of algorithmic self-assembly. *Communications of the ACM*, 55(12):78–88, 2012.
5. Cody Geary, Pierre-Étienne Meunier, Nicolas Schabanel, and Shinnosuke Seki. Efficient universal computation by greedy molecular folding. CoRR abs/1508.00510, 2015.
6. Cody Geary, Pierre-Étienne Meunier, Nicolas Schabanel, and Shinnosuke Seki. Programming biomolecules that fold greedily during transcription. In *Proc. 41st International Symposium on Mathematical Foundations of Computer Science (MFCS2016)*, Leibniz International Proceedings in Informatics (LIPIcs) 58, pages 43:1–43:14, 2016.

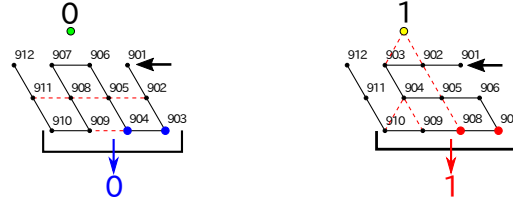


Fig. 16. The possible two conformations of body-lpx2 component.

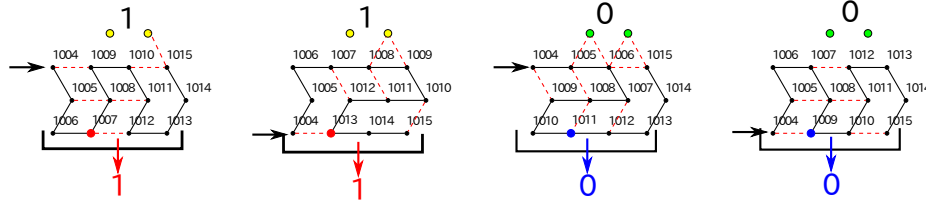


Fig. 17. The possible four conformations of body-gx component.

7. Cody Geary, Paul W. K. Rothmund, and Ebbe S. Andersen. A single-stranded architecture for cotranscriptional folding of RNA nanostructures. *Science*, 345(6198):799–804, 2014.
8. Yo-Sub Han and Hwee Kim. Ruleset optimization on isomorphic oritatami systems. In *Proc. 23rd International Conference on DNA Computing and Molecular Programming (DNA23)*, LNCS. Springer, 2017. in press.
9. Yo-Sub Han, Hwee Kim, Makoto Ota, and Shinnosuke Seki. Nondeterministic seedless oritatami systems and hardness of testing their equivalence. In *Proc. 22nd International Conference on DNA Computing and Molecular Programming (DNA22)*, volume 9818 of *LNCS*, pages 19–34. Springer, 2016.
10. Jun Ma and Judy Holdener. When Thue-Morse meets Koch. *Fractals*, 13:191–206, 2005.
11. Yusei Masuda, Shinnosuke Seki, and Yuki Ubukata. The simulator of heighway dragon.
12. Makoto Ota and Shinnosuke Seki. Ruleset design problems for oritatami systems. *Theoretical Computer Science*, 671:26–35, 2017.
13. Matthew J. Patitz. Self-assembly of fractals. In *Encyclopedia of Algorithms*, pages 1918–1922. Springer, 2016.
14. Matthew J. Patitz and Trent A. Rogers. Personal Communication.
15. Paul W. K. Rothmund, Nick Papadakis, and Erik Winfree. Algorithmic self-assembly of DNA Sierpinski triangle. *PLoS Biology*, 2(12):e424, 2004.
16. Kyle E. Watters, Eric J. Strobel, Angela M. Yu, John T. Lis, and Julius B. Lucks. Cotranscriptional folding of a riboswitch at nucleotide resolution. *Nature Structural & Molecular Biology*, 23(12):1124–1133, 2016.
17. Erik Winfree. *Algorithmic Self-Assembly of DNA*. PhD thesis, California Institute of Technology, June 1998.

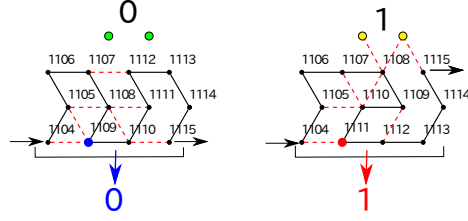


Fig. 18. The possible two conformations of body-rgy component.

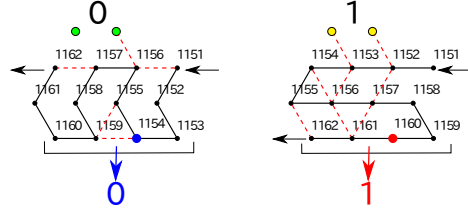


Fig. 19. The possible two conformations of body-lgy component.

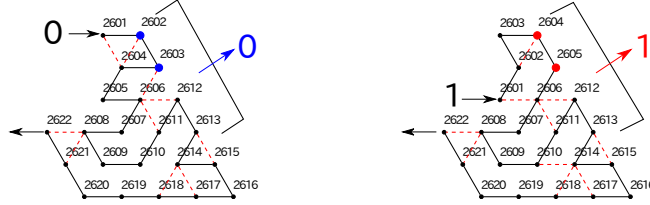


Fig. 20. The possible two conformations of turn-rgp component.

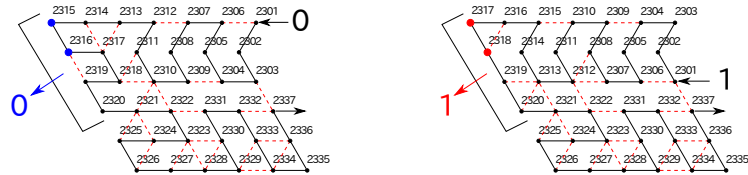


Fig. 21. The possible two conformations of turn-lgp component.

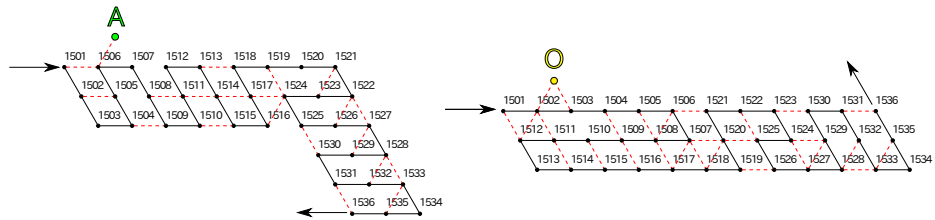


Fig. 22. The possible two conformations of change-route component.



Fig. 23. The possible two conformations of move component.